

Supporting information

Unravelling moisture-induced CO₂ chemisorption mechanisms in amine-modified silica sorbents at the molecular scale

Mariana Sardo,^{a,*} Rui Afonso,^a Joanna Juzków,^a Marlene Pacheco,^b Marta Bordonhos,^b Moisés L. Pinto,^b José R.B. Gomes^a and Luís Mafra^{a,*}

^a CICECO - Aveiro Institute of Materials, Department of Chemistry, University of Aveiro, Campus Universitário de Santiago, 3810-193 Aveiro, Portugal

^b CERENA, Instituto Superior Técnico, University of Lisbon, Av. Rovisco Pais, 1049-001 Lisboa, Portugal

TABLE OF CONTENTS

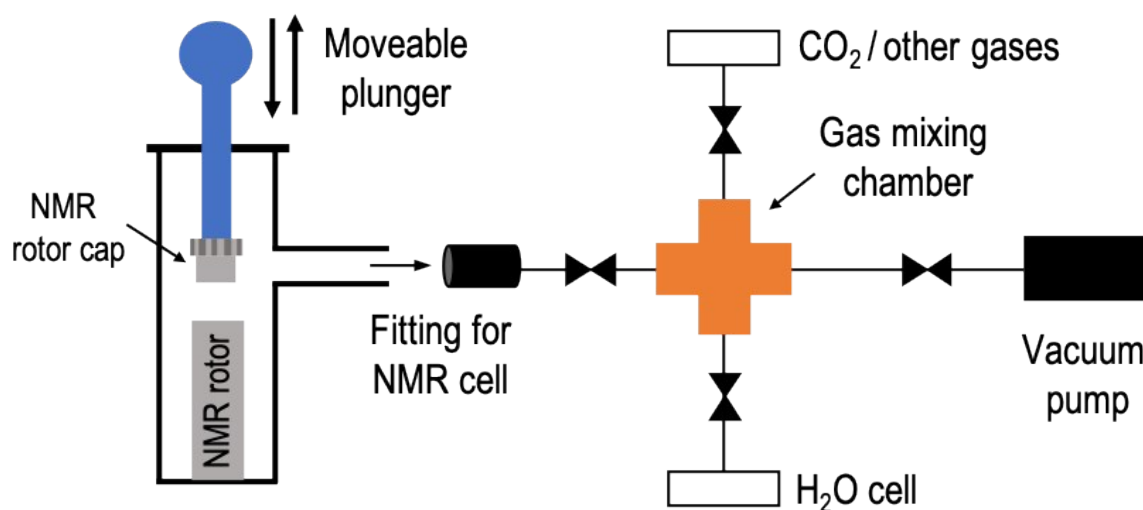
Materials Characterization	2
Scheme S1. Home-built vacuum line.....	2
Table S1. Textural properties	3
Table S2. Calculated Gibbs energy	3
Table S3. Calculated ¹³ C NMR chemical shifts	4
Figure S1. Nitrogen adsorption isotherms.....	5
Figure S2. FTIR spectra	5
Figure S3. Thermal analysis.....	6
Figure S4. ¹³ C solid-state NMR spectra.....	7
Figure S5. 3D structure models for carbamic acid and ammonium carbamate species.....	7
Figure S6. 3D structure model exhibiting the ¹ H resonance at 7.2 ppm.....	8
Figure S7. ¹ H- ²⁹ Si CPMAS HETCOR NMR spectrum.....	8
Figure S8. Model and calculated ¹ H NMR CS	9
Test of the computational strategy	9
Scheme S2. 2D models	9
Table S4. Comparison of experimental and calculated ¹ H and ¹³ C shifts for species A	10
Table S5. Comparison of experimental and calculated ¹ H and ¹³ C shifts for species B	11
Table S6. Comparison of experimental and calculated ¹ H and ¹³ C shifts for species C	11
Table S7. Differences in the ¹³ C shifts.....	12

Materials Characterization – Experimental Details

The porous texture characterization of the materials was made by N₂ adsorption at −196 °C. The N₂ adsorption isotherms were obtained in an automatic apparatus Micromeritics ASAP 2010. Before the isotherms measurement, the samples (~50 mg) were outgassed during 2.5 h at 150 °C under vacuum greater than 10^{−2} Pa. From N₂ adsorption data the specific surface area (A_{BET}) was determined through Brunauer–Emmett–Teller (BET) equation in the $0.05 < p/p^o < 0.2$ pressure range,¹ and the total pore volume (V_{total}) was assessed by the Gurvich rule,¹ corresponding to the volume of N₂ adsorbed at $p/p^o = 0.95$. The mesopore size distributions were obtained by the Broekhoff–de Boer method, in a version simplified with the Frenkel–Halsey–Hill equation² that was previously shown to give accurate results when applied to mesoporous silicas and silicates.³

Thermogravimetry with differential scanning calorimetry (TG-DSC) experiments were carried out in an apparatus (Setaram TG- DSC 111) with 0.001 mg and 0.05 mW of precision, using about 10 mg samples, between 25 and 600 °C, under dry air flux (Air Liquid). From the mass loss between 150 and 500 °C, the organic content of samples was determined. This temperature range corresponded to the exothermic peaks observed on the heat flow curves, assigned to the decomposition of the organic linkers in air.

Elemental analysis was performed on a Truspec 630-200-200 equipment, using infrared absorption as the detection method for Carbon and Hydrogen and thermal conductivity for nitrogen (combustion temperature of 1075 °C).

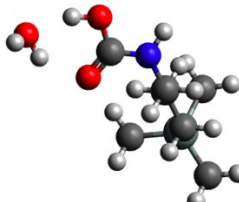
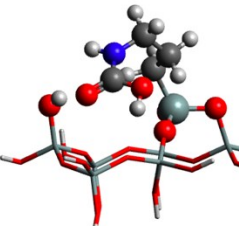
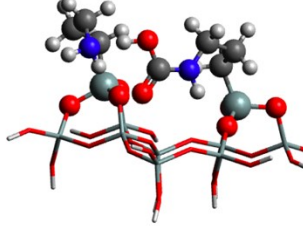
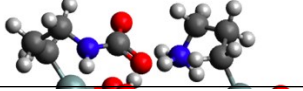


Scheme S1. Home-built vacuum line for degassing and loading NMR samples with ¹³CO₂ and water vapor.

Table S1. Textural properties: surface area (A_{BET}), total pore volume from adsorbed amounts at 0.9 p/p^0 (V_{pore}), pore diameter (d_{pore}), nitrogen content and grafting density of the samples.

Sample	A_{BET} $\text{m}^2 \text{g}^{-1}$	V_{pore} $\text{cm}^3 \text{g}^{-1}$	d_{pore} nm	N content mmol/g
SBA-15	743 ± 3	0.839	7.0	-
DEAPTES@SBA-15	329 ± 3	0.585	7.0	1.00
APTES@SBA-15	340 ± 2	0.665	7.8	1.08

Table S2. Calculated Gibbs energy differences of CO_2 species formed on primary amines, with the corresponding clusters.

Conditions	Species	ΔG ($\text{kJ} \times \text{mol}^{-1}$)	Model
1-amine			
Dry	Adsorbed CO_2	6	
	Carbamic acid	0	
Wet	Adsorbed CO_2 and H_2O	29	
	Bicarbonate/Carbonic acid	15	
	Carbamic acid	0	
1-amine and 1-silanol			
Dry	Adsorbed CO_2	15	
	Carbamic acid	0	
Wet	Adsorbed CO_2 and H_2O	26	
	Bicarbonate/Carbonic acid	3	
	Carbamic acid	0	
2-amines			
Dry	Adsorbed CO_2	42	
	Carbamic acid	0	
Wet	Adsorbed CO_2 and H_2O	30	
	Bicarbonate/Carbonic acid	10	
	Carbamic acid	0	
2-amines and 1-silanol			
Dry	Adsorbed CO_2	43	
	Ammonium Carbamate	4	

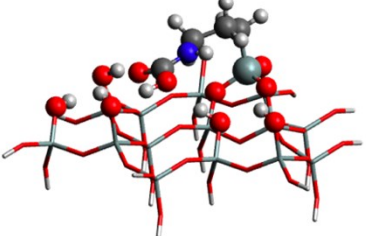
	Carbamic acid	0	
Wet	Adsorbed CO ₂ and H ₂ O	68	
	Bicarbonate/Carbonic acid	45	
	Carbamic Acid	29	
	Ammonium Carbamate	0	
1-amine and 5-silanols			
Dry	Adsorbed CO ₂	27	
	Carbamic acid	0	
Wet	Adsorbed CO ₂ and H ₂ O	46	
	Carbamic acid	7	
	Bicarbonate/Carbonic acid	0	

Table S3. Calculated ¹³C NMR chemical shifts under dry and humid conditions for the CO₂ species formed in primary amines, for different cluster models.

Dry	Carbamic Acid	Ammonium Carbamate	
1-amine	154.0	—	
1-amine and 1-silanol	158.2	—	
2-amines	161.8	—	
2-amines and 1-silanol	159.3	163.7	
1-amine and 5-silanols	156.1	—	
Wet	Carbamic Acid	Ammonium Carbamate	Bicarbonate
1-amine	159.7	—	158.2
1-amine and 1-silanol	161.7	—	159.9
2-amines	163.4	—	162.6
2-amines and 1-silanol	158.5	166.0	164.6
1-amine and 5-silanols	158.2	—	160.7

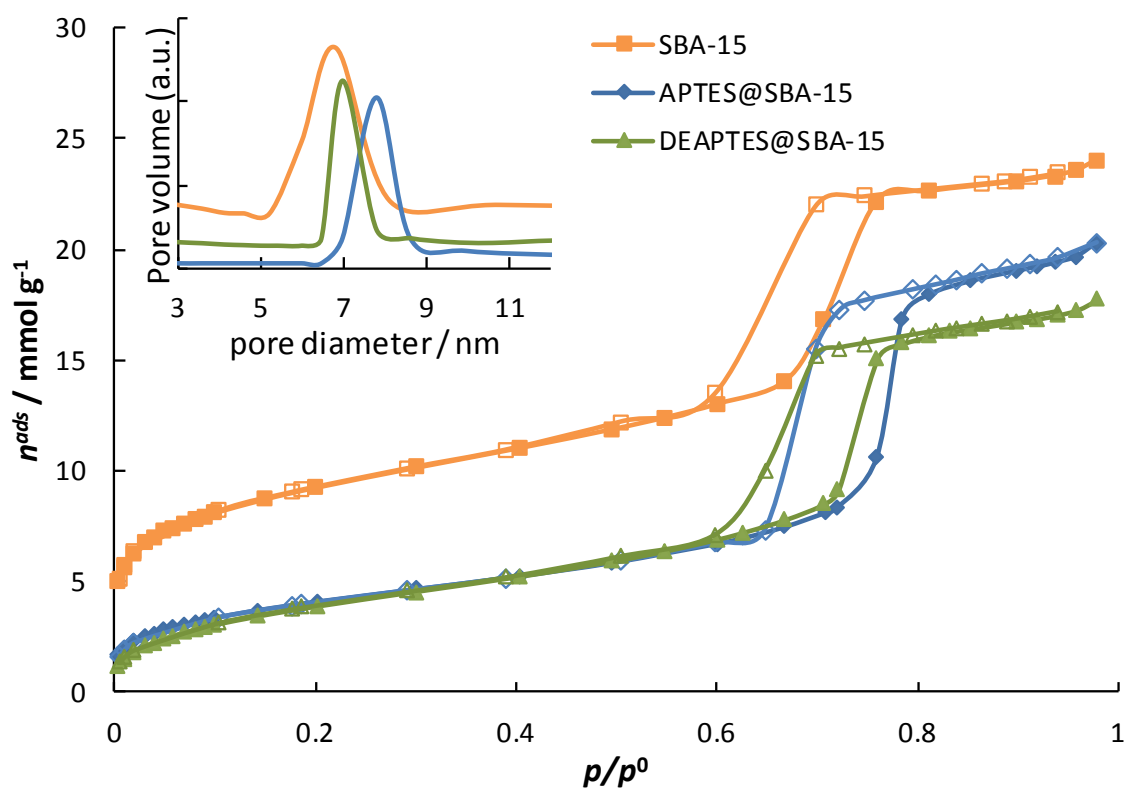


Figure S1. Nitrogen adsorption isotherms at -196°C.

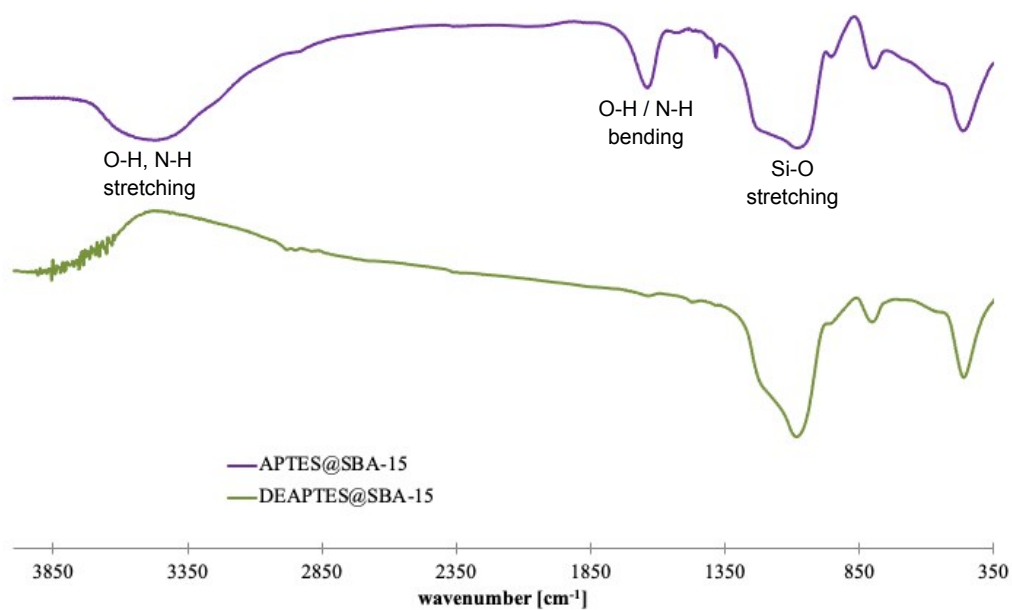


Figure S2. FTIR spectra of the samples APTES@SBA-15 and DEAPTES@SBA-15.

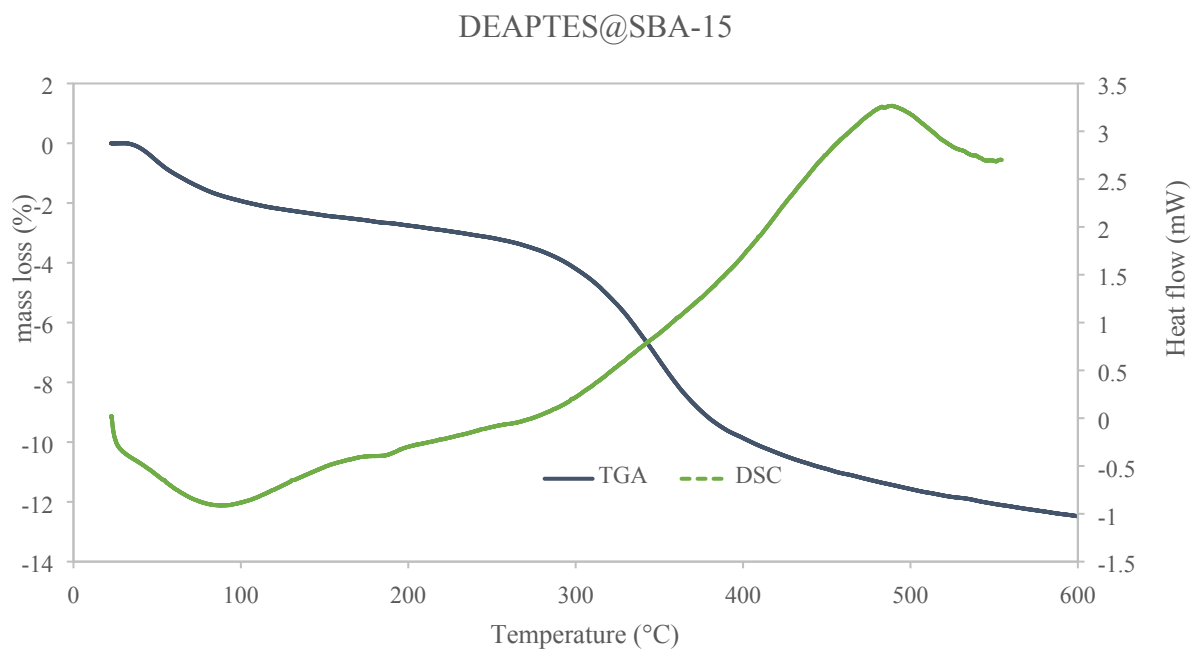
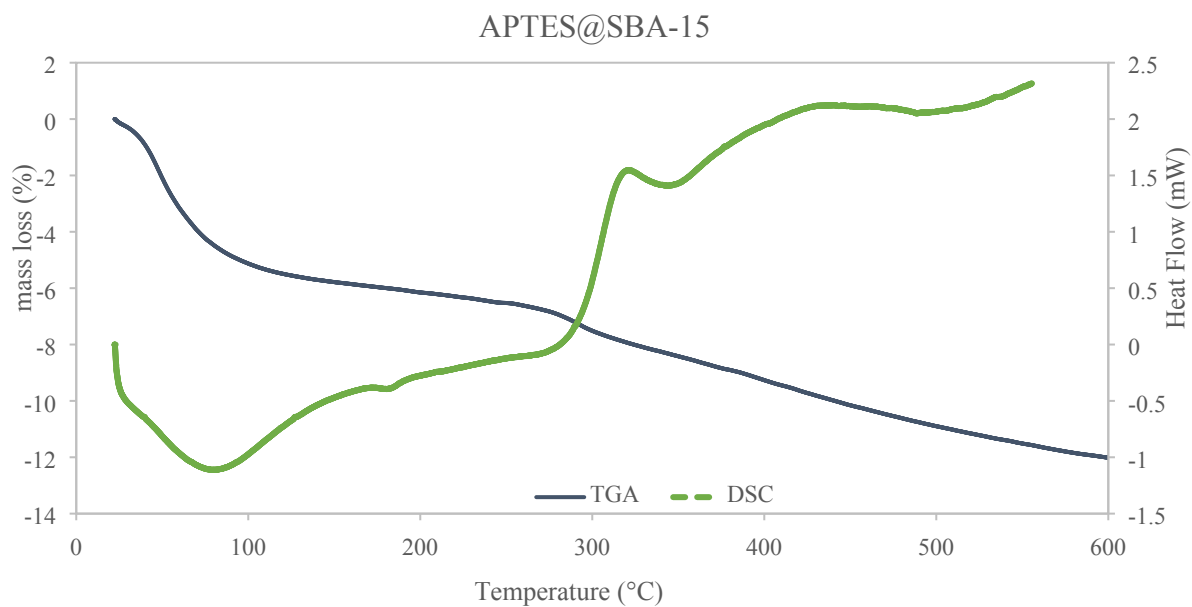


Figure S3. Thermal analysis (TGA and DSC) of the samples APTES@SBA-15 (top) and DEAPTES@SBA-15 (bottom).

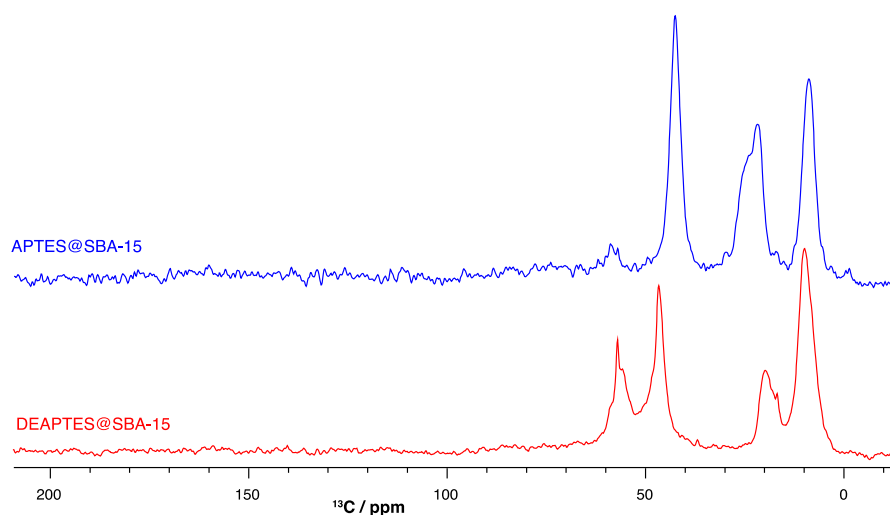


Figure S4. ^{13}C solid-state NMR spectra of DEAPTES@SBA-15 and APTES@SBA-15 samples.

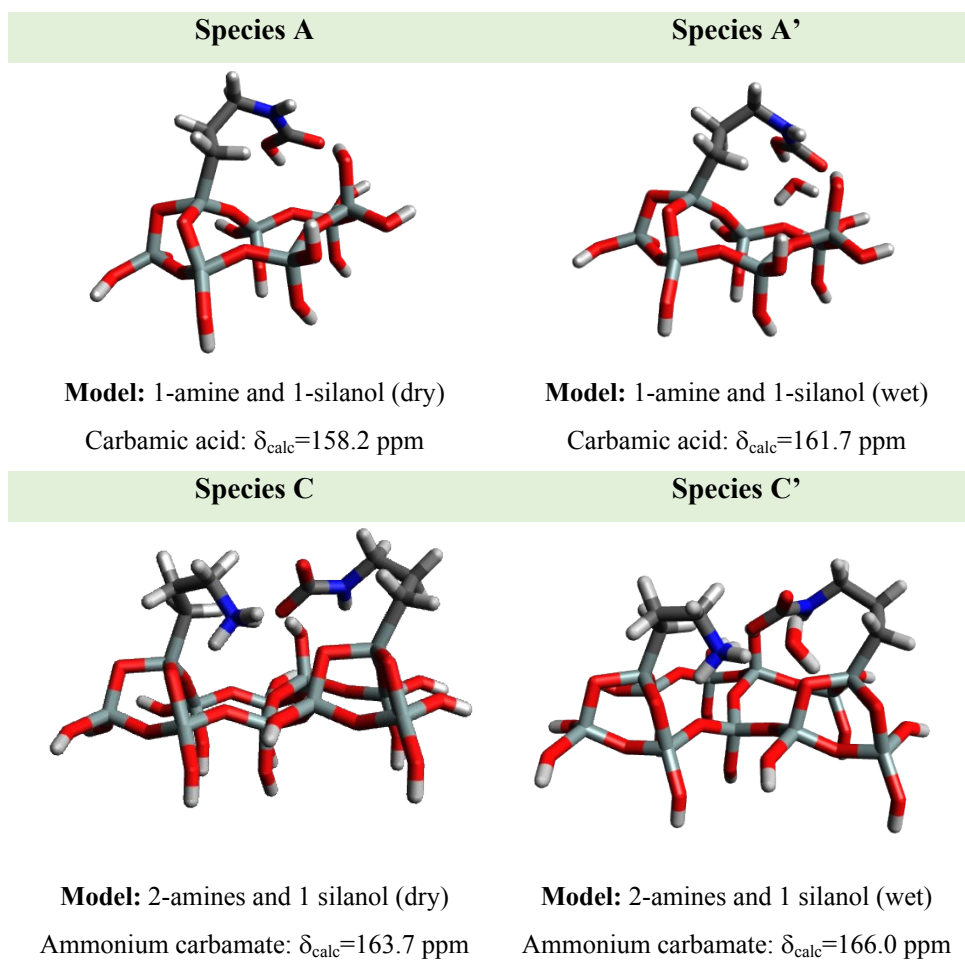


Figure S5. 3D structure models for carbamic acid and ammonium carbamate species formed in primary amines under wet and dry conditions. (chemical shifts calculated for each model are displayed in Table S2 and Gibbs energy in Table S1)

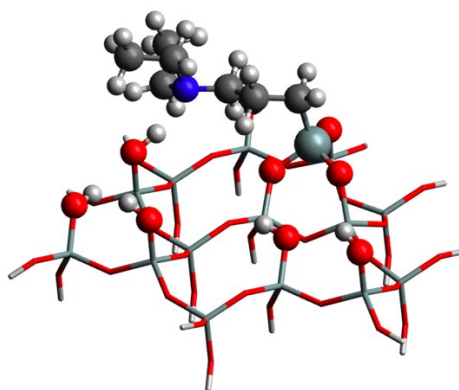


Figure S6. 3D structure model exhibiting the ^1H resonance at 7.2 ppm (hydrogen atom interacting with the nitrogen atom from the amine).

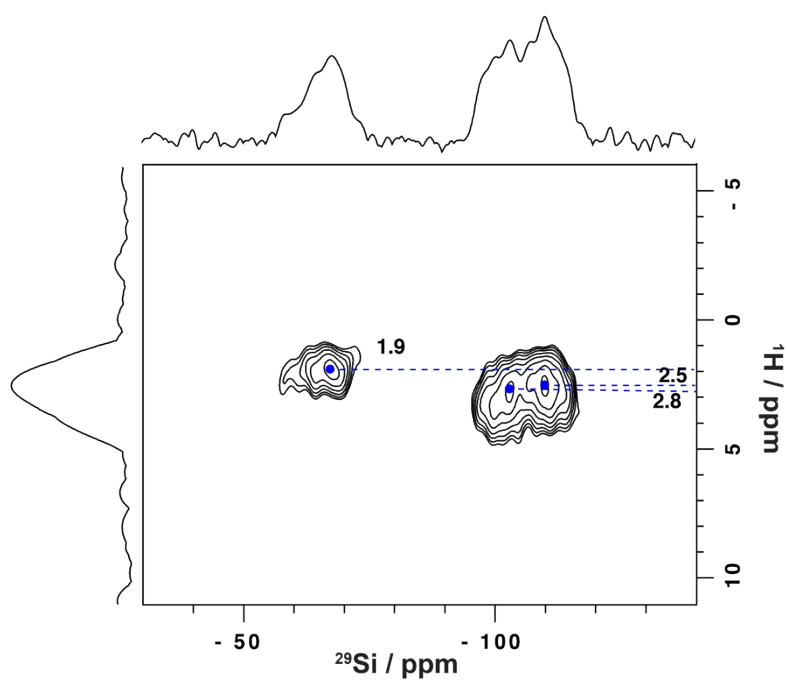


Figure S7. ^1H - ^{29}Si CPMAS HETCOR NMR spectrum of DEAPTES@SBA-15 exposed to 2.7 kPa of water vapor and 100 kPa of $^{13}\text{CO}_2$, recorded at 9.4 T with a spinning rate of 10 kHz and using a contact time of 8 ms. Additional parameters provided in the experimental section.

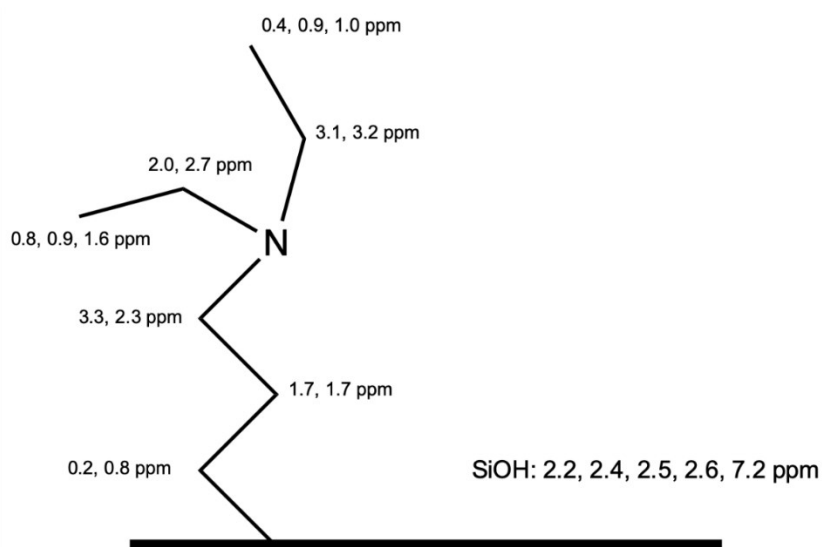
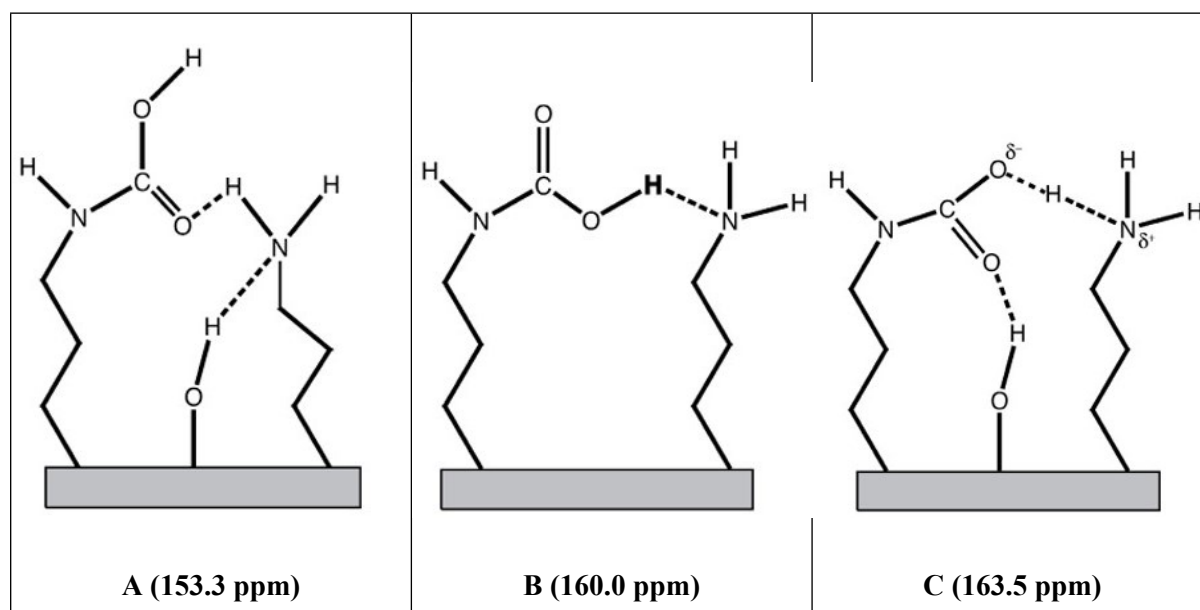


Figure S8. Model and calculated ^1H NMR CS values for isolated DEAPTES.

Test of the computational strategy

The structures A, B and C (Scheme S2), formed upon CO_2 adsorption by APTES@SBA-15 reported in our previous work,⁴ i.e., structures with ^{13}C of the adsorbed carbon species appearing at ~ 153 ppm, 160 ppm and 163.5 ppm, respectively, were used to understand the influence of the basis set size in the quality of the calculated NMR shifts.



Scheme S2. 2D models of the carbonaceous species suggested to form upon CO_2 adsorption by APTES@SBA-15.

All calculations considered the M062X functional since this is the functional suggested in the computational protocol by Willoughby *et al.*,⁵ for small-molecule structure assignment through computation of ¹H and ¹³C NMR chemical shifts. The following combinations of basis sets for NMR calculation/geometry optimization runs were considered:

6-31G*/6-31G* (**BS A**);

6-31G**/6-31G** (**BS B**);

6-31+G**/6-31+G** (**BS C**);

6-311++G**/6-311++G** (**BS D**);

6-311++G**/6-31G** (**BS E**); and

6-311+G(2d,p)/6-31+G** (**BS F**).

The calculated ¹³C and ¹H shifts reported for the three carbonaceous species, using TMS (tetramethylsilane) calculated at the same levels of theory as the reference, are compiled in the Tables below.

Table S4. Comparison of experimental and calculated ¹H and ¹³C shifts for species **A** using the M062X functional and several different basis sets. All values in ppm.

atom	BS A	BS B	BS C	BS D	BS E	BS F	Exptl.
H	0.6	1.1	0.6	0.3	0.3	0.3	1 – 5
H	2.6	3.4	2.8	2.6	2.9	2.6	(cluttered region)
H	4.0	4.8	4.8	4.6	4.5	4.5	
H	4.5	5.1	5.1	5.1	5.1	4.8	
H	9.6	11.6	11.4	10.5	11.4	11.1	8.4
C	154.2	156.0	160.0	167.1	168.3	168.8	153.3
t(NMR) ^a	1.00	1.16	5.10	12.89	15.16	17.80	

^at(NMR) is the time taken by the NMR calculation only (without optimization) using the basis set in the top row divided by the time taken by the NMR calculation with BS A. Smaller time for combination BS D than combination BS E is due to the reading of the optimized wave function from the optimization step at the same level of theory.

Table S5. Comparison of experimental and calculated ^1H and ^{13}C shifts for species **B** using the M062X functional and several different basis sets. All values in ppm.

atom	BS A	BS B	BS C	BS D	BS E	BS F	Exptl.
H	0.5	1.1	0.9	0.7	0.7	0.9	1 – 5
H	2.2	2.9	2.8	2.9	2.9	2.7	(cluttered region)
H	3.3	4.1	4.1	4.1	4.1	4.0	
H	12.8	14.7	14.7	14.6	14.5	14.5	
C	160.5	162.2	165.6	175.3	175.0	174.6	160.0
t(NMR) ^a	1.00	1.16	5.11	10.85	14.58	16.17	

^at(NMR) is the time taken by the NMR calculation only (without optimization) using the basis set in the top row divided by the time taken by the NMR calculation with BS A. Smaller time for combination BS D than combination BS E is due to the reading of the optimized wave function from the optimization step at the same level of theory.

Table S6. Comparison of experimental and calculated ^1H and ^{13}C shifts for species **C** using the M062X functional and several different basis sets. All values in ppm.

atom	BS A	BS B	BS C	BS D	BS E	BS F	Exptl.
H	0.5	1.1	0.8	0.8	0.8	0.7	1 – 5
H	0.7	1.2	0.9	0.9	0.8	0.7	(cluttered region)
H	4.0	4.9	4.7	4.5	4.5	2.3	
H	4.3	5.3	5.1	5.0	5.0	5.0	
H	12.3	14.1	13.9	14.0	13.9	13.6	7.3 (8.8)
C	163.1	164.8	168.4	177.6	177.4	177.6	163.5
t(NMR) ^a	1.00	1.16	5.23	12.53	14.23	17.70	

^at(NMR) is the time taken by the NMR calculation only (without optimization) using the basis set in the top row divided by the time taken by the NMR calculation with BS A. Smaller time for combination BS D than combination BS E is due to the reading of the optimized wave function from the optimization step at the same level of theory.

As it can be seen from Tables S4-S6, without any additional correction scheme, the results calculated with BS A compare very well with the available experimental results (including that for gaseous CO_2 , 125 ppm against TMS, not shown) while the increase of the basis set leads to a systematic overestimation of the calculated shifts when comparing to those calculated with BS A. Nevertheless, the difference of the shifts for the ^{13}C species, ongoing from Species **A** to **B** and from Species **B** to **C** are very similar when considering any of the basis sets (Table S7 below).

Table S7. Differences in the ^{13}C shifts, with $\text{D1} = {}^{13}\text{C}_{(\text{species B})} - {}^{13}\text{C}_{(\text{species A})}$ and with $\text{D2} = {}^{13}\text{C}_{(\text{species C})} - {}^{13}\text{C}_{(\text{species B})}$. All values in ppm.

Difference	BS A	BS B	BS C	BS D	BS E	BS F	Exptl.
D1	6.2	6.2	5.6	8.1	6.7	5.8	6.7
D2	2.7	2.6	2.8	2.4	2.4	2.9	3.5

Therefore, if a suitable reference is used, any combination of basis sets will lead essentially to the same results, hence, the main difference being the computational time that, obviously, increases with the basis set size. The increase in the computational time assumes a huge importance when calculating systems with many atoms as those in the present study, and where many different conformations had to be analyzed.

Other studies in the literature show also that the accuracy of the calculated NMR shifts is not increased by the increase of the basis set size. This is the case of the work by Hehre *et al.*⁶ where it was analyzed the influence of increasing the size of the basis set from 6-31G* to 6-31G**, to 6-311G*, to 6-311G**, and to 6-311G(2d,2p) in the calculated ^{13}C shifts of strychnine, with all calculations performed with the $\omega\text{B97X-D}$ exchange-correlation functional. Also, in the study by Flaig *et al.*⁷ it was found that the consideration of 6-31G**, 6-311G** or def2-TZVPP basis sets and the same DFT functional leads to very similar standard deviations of calculated ^1H or ^{13}C shifts of several different organic molecules. These two examples taken from the literature also support that bigger (basis size) is not better (accuracy of NMR shifts).

References

- 1 J. Rouquerol, F. Rouquerol, P. Llewellyn, G. Maurin and K. Sing, *Adsorption by powders and porous solids : principles, methodology and applications*, San Diego, 1999.
- 2 J. Wayne W. Lukens, P. Schmidt-Winkel, D. Zhao, J. Feng and G. D. Stucky, *Langmuir*, 1999, **15**, 5403–5409.
- 3 J. Pires, A. Carvalho, M. Pinto and J. Rocha, *J. Porous Mater.*, 2006, **13**, 107–114.
- 4 P. H. Willoughby, M. J. Jansma and T. R. Hoye, *Nat. Protoc.*, 2014, **9**, 643–660.
- 5 W. Hehre, P. Klunzinger, B. Deppmeier, A. Driessen, N. Uchida, M. Hashimoto, E. Fukushi and Y. Takata, *J. Nat. Prod.*, 2019, **82**, 2299–2306.
- 6 D. Flaig, M. Maurer, M. Hanni, K. Braunger, L. Kick, M. Thubauville and C. Ochsenfeld, *J. Chem. Theory Comput.*, 2014, **10**, 572–578.